Lung Inhomogeneities and Time Course of Ventilator-induced Mechanical Injuries

Massimo Cressoni, M.D., Chiara Chiurazzi, M.D., Miriam Gotti, M.D., Martina Amini, M.D., Matteo Brioni, M.D., Ilaria Algieri, M.D., Antonio Cammaroto, M.D., Cristina Rovati, M.D., Dario Massari, M.D., Caterina Bacile di Castiglione, M.D., Klodiana Nikolla, M.D., Claudia Montaruli, M.D., Marco Lazzerini, M.D., Daniele Dondossola, M.D., Angelo Colombo, M.D., Stefano Gatti, M.D., Vincenza Valerio, Ph.D., Nicoletta Gagliano, Ph.D., Eleonora Carlesso, M.Sc., Luciano Gattinoni, M.D., F.R.C.P.

ABSTRACT

Background: During mechanical ventilation, stress and strain may be locally multiplied in an inhomogeneous lung. The authors investigated whether, in healthy lungs, during high pressure/volume ventilation, injury begins at the interface of naturally inhomogeneous structures as visceral pleura, bronchi, vessels, and alveoli. The authors wished also to characterize the nature of the lesions (collapse *vs.* consolidation).

Methods: Twelve piglets were ventilated with strain greater than 2.5 (tidal volume/end-expiratory lung volume) until whole lung edema developed. At least every 3 h, the authors acquired end-expiratory/end-inspiratory computed tomography scans to identify the site and the number of new lesions. Lung inhomogeneities and recruitability were quantified.

Results: The first new densities developed after 8.4 ± 6.3 h (mean ± SD), and their number increased exponentially up to 15 ± 12 h. Afterward, they merged into full lung edema. A median of 61% (interquartile range, 57 to 76) of the lesions appeared in subpleural regions, 19% (interquartile range, 11 to 23) were peribronchial, and 19% (interquartile range, 6 to 25) were parenchymal ($P < 0.0001$). All the new densities were fully recruitable. Lung elastance and gas exchange deteriorated significantly after 18 ± 11 h, whereas lung edema developed after 20 ± 11 h.

Conclusions: Most of the computed tomography scan new densities developed in nonhomogeneous lung regions. The damage in this model was primarily located in the interstitial space, causing alveolar collapse and consequent high recruitability.
(Anesthesiology 2015; 123:618-27)

"Higher" tidal volumes (12 ml/kg) lead to dismal outcome when used to ventilate patients with adult respiratory distress syndrome (ARDS)[1,2] and normal subjects during anesthesia,[3] compared with "lower" tidal volumes (6 ml/kg). Therefore, the high-volume mechanical ventilation is recognized as the primary determinant of ventilator-induced lung injury (VILI), although other factors such as increased flow, pulmonary vascular pressure,[4–6] and temperature[7] may be involved. Experimental studies consistently showed that in normal lungs, it was possible to induce VILI up to death by using extremely large tidal volumes,[8] from 40 to 70 ml/kg,[9,10] three to fourfold the 12 ml/kg tidal volume found harmful in ARDS.[1]

What We Already Know about This Topic

- Excessive stress and strain induce lung injury.

What This Article Tells Us That Is New

- Ventilator-induced lung injury detected as an increased density on computed tomography scan, first occurred at inhomogeneous interfaces, including at the visceral pleura and at the subpleural alveolar walls in anesthetized piglets ventilated with a tidal volume/end-expiratory lung volume more than 2.5. New lung densities were found within 8 h of the ventilation and their number increased exponentially up to 15 h. Lung elastance and gas exchange deteriorated significantly after 18 h and full lung edema developed after 20 h.

Supplemental Digital Content is available for this article. Direct URL citations appear in the printed text and are available in both the HTML and PDF versions of this article. Links to the digital files are provided in the HTML text of this article on the Journal's Web site (www.anesthesiology.org). This study was presented at the International Symposium on Intensive Care and Emergency Medicine, Brussels, Belgium, March 18, 2014; and the 27th European Society of Intensive Care Medicine Congress, Barcelona, Spain, October 1, 2014.

Submitted for publication October 7, 2014. Accepted for publication March 31, 2015. From the Dipartimento di Fisiopatologia Medico-Chirurgica e dei Trapianti, Fondazione IRCCS Ca' Granda-Ospedale Maggiore Policlinico, Università degli Studi di Milano, Milan, Italy (M.C., C.C., M.G., M.A., M.B., I.A., A. Cammaroto, C.R., D.M., C.B.d.C., K.N., C.M., E.C.); Dipartimento di Radiologia, Fondazione IRCCS Ca' Granda-Ospedale Maggiore Policlinico, Milan, Italy (M.L.); Centro di Ricerche Precliniche, Fondazione IRCCS Ca' Granda-Ospedale Maggiore Policlinico, Milan, Italy (D.D., S.G.); Dipartimento di Anestesia, Rianimazione ed Emergenza Urgenza, Fondazione IRCCS Ca' Granda-Ospedale Maggiore Policlinico, Milan, Italy (A. Colombo, L.G.); and Dipartimento di Scienze Biomediche per la Salute, Università degli Studi di Milano, Milan, Italy (V.V., N.G.).

 Anesthesiology 2015; 123:618-27

To explain the huge tidal volume difference to induce VILI in healthy and diseased lungs, two theories have been proposed: the "second hit" hypothesis[11–15] and the "stress raiser" theory.[16] According to the "second hit" hypothesis, stimuli from mechanical ventilation and activation of the inflammatory cascade induced by the primary disease do not have an addictive but a multiplicative effect. Consequently, a mechanical ventilation, safe in healthy lungs, may be deleterious if applied to an inflamed parenchyma. Although this theory may well fit with the ARDS lung, it is more difficult to conceptualize it in a noninflamed lung during anesthesia, where VILI may be present.

The stress raiser theory, instead of biological reaction, is purely founded on mechanics.[16,17] Accordingly, a given pressure/volume applied to an inhomogeneous region may locally induce a stress concentration as the interfaces act as "stress raisers." This theory too applies to ARDS where patchy inflammatory reactions may behave as inhomogeneities but may be also applied to a noninflamed lung where structural modifications, occurring, as an example, with age, may act as stress raisers. To recognize and measure lung inhomogeneities may be of clinical relevance when tailoring mechanical ventilation.[17] Unfortunately, however, we still lack a proof of a cause–effect relationship between lung inhomogeneities and damages of mechanical ventilation, which would support the stress raiser theory.

We reasoned that, if the inhomogeneities act as stress raisers in normal lung, the VILI should first appear where inhomogeneities are physiologically present as at pleura/alveoli interface[18] and around bronchi and vessels. Therefore, to investigate the cause–effect relationship between VILI and stress raiser, we maximized the tidal volume to obtain the effects in a reasonable amount of time (54 h).[19] In addition, we chose healthy animals to avoid other confounding factors. By chance, however, half of the experimental animals that presented as normal actually had pathologic densities at the first computed tomography (CT) scan; consequently, we had the opportunity to study the VILI progression associated with physiologic and pathologic inhomogeneities.

Therefore, we studied 12 piglets, ventilated in a prone position with extremely high tidal volume (lung strain greater than 2.5) to verify: (a) if the lung lesions first appear in the regions of physiologic/pathologic inhomogeneities; (b) the "nature" of these VILI lesions (consolidated or collapsed tissue); (c) the time course of the VILI lesions and their relationship with anatomical, respiratory, hemodynamic, and gas exchange variables.

Materials and Methods

We studied 12 large, white female piglets (22 ± 5 kg) apparently healthy. Six of them, however, at the first CT scan, presented the regions of abnormal density that were unrecruitable (7.5 ± 6% of total lung volume at end inspiration, defined as "consolidated tissue," see Supplemental Digital Content 1, fig. 4, http://links.lww.com/ALN/B158). The animals that had baseline normal physiologic variables (gas exchange, respiratory mechanics, and hemodynamics) were included in the study to verify whether VILI developed at interface between these densities and the surrounding parenchyma. This study was approved by Italian Board of Health (Ministero della Salute, Direzione Generale della Sanità Animale e dei farmaci veterinari, Roma, Italy) and was performed according to the Helsinki convention for the use and care of animals and complied with the international recommendations.[20]

Measured Variables

Piglets were fully instrumented (orotracheal tube, esophageal balloon, central venous pressure, arterial line, and urinary catheter). The following variables were recorded/computed (Colligo, Elekton, Italy)[21]: respiratory variables: tidal volume, peak, plateau and expiratory airway and esophageal pressures, chest and lung elastances; gas exchange variables: Pa_{O_2}, Pa_{CO_2}, pH, lactates, hemoglobin concentration, and saturation; hemodynamics: arterial and central venous pressure, urinary output, fluid intake, and cardioactive drugs; and CT scan variables: lung weight; lung gas volume; over, normally, poorly, and not inflated lung tissue; and lung recruitment, defined as the percentage of lung tissue that regains inflation between end expiration and end inspiration[22] (see Additional Methods in Supplemental Digital Content 1, http://links.lww.com/ALN/B158).

Pathology

Lung fragments were obtained from each region of both lungs (see Supplemental Digital Content 1, fig. 2, http://links.lww.com/ALN/B158): three samples from subpleural regions, one sample from the medial surface of the lung, taken cutting the lung parallel to the main bronchus and excising the sample from the medial surface of the lung. The lung regions used for histology did not correspond to the six lung fields used for CT scan analysis, as we compared the periphery of the lung with the "core" of the lung. After processing the samples, the following variables were measured: hyaline membranes, interstitial and septal infiltrates, vascular congestion and intra-alveolar hemorrhaging, alveoli rupturing, and basophilic material deposition. Overall injury was expressed by a scoring system from 0 to 4: 0, no alterations; 1, 25% of field involved; 2, 50% of field involved; 3, 75% of field involved; and 4, 100% of field involved. Collagen and elastin content were expressed as a percent of the stained area relative to the lung tissue.

Lung Inhomogeneities

We applied the method previously used in human,[17] but scaling the acinus dimension to piglet size (see Supplemental Digital Content 1, fig. 5, http://links.lww.com/ALN/B158). Lung inhomogeneities were computed by comparing the gas fraction of each voxel with the gas fraction of the surrounding voxels. The ratio of the latter to the former equal to 1 indicates

homogeneity and greater than 1 indicates inhomogeneity. We used as a threshold the values of 95th percentile of lung inhomogeneities measured in our healthy piglets at baseline (threshold of 1.685) and expressed the inhomogeneity values as intensity (average ratio) and extent (fraction of lung volume above the 95th percentile of lung inhomogeneities).

Study Protocol

After a recruitment maneuver, piglets were ventilated in prone position with a tidal volume/functional residual capacity ratio (strain) greater than 2.5 (38 ± 4.6 ml/kg), at respiratory rate of 15 breaths/min, zero end-expiratory pressure (zero positive end-expiratory pressure), I:E of 1:2, and F_{IO_2} of 0.5 (see Supplemental Digital Content 1, fig. 1, http://links.lww.com/ALN/B158). Functional residual capacity for the strain computation was determined with CT scan. Two CT scans (end expiration and end inspiration) and a complete set of physiological variables were collected. End expiratory and end inspiratory CT scans were scheduled every 3 h and all the other variables every 6 h, unless a variation occurred either on CT scan or in physiologic variables. In both cases, a complete set of new measurements was collected. The study was interrupted after a whole lung edema developed. After the experiment, the lung wet-to-dry ratios were determined and samples for histology collected in eight different lung regions (see Supplemental Digital Content 1, fig. 2, http://links.lww.com/ALN/B158).

CT Scan Time Course

New densities were classified as subpleural (adjacent to the pleura), peribronchial (bronchogram clearly identifiable inside or adjacent to the new density), and parenchymal (not adjacent to the pleura, without a bronchogram), see Supplemental Digital Content 1, figure 3, http://links.lww.com/ALN/B158. The localization of new densities was classified in six predefined lung fields (apex/hilum/base, dependent/nondependent).

The densities were classified on end-expiration CT scans by three independent observers (M.G., C.C., and M.L.). The three independent observers were not blinded, and images were presented in the same time sequence they were acquired. The interobserver variability in counting densities was 5%. We classified the densities as (a) new densities: regions of density clearly distinguishable from the remaining parenchyma; (b) one-field edema: density occupying at least one lung field; with one-field edema densities were distinguishable in the other fields (see Supplemental Digital Content 1, fig. 12, http://links.lww.com/ALN/B158); and (c) all-field edema: density occupying all the six lung fields. To classify their evolution, we defined the following time points: Time 0, the baseline CT scan; Time 1, the last CT scan without new densities; Time 2, the first CT scan with new densities; Time 3, the last CT scan with distinguishable densities; Time 4, the first CT scan with one-field edema; and Time 5, the first CT scan with all-field edema.

Statistical Analysis

The location of densities and variables at the six time points considered were compared with a mixed model (lme function of the nlme library); Bonferroni correction was used for multiple comparisons. The behavior of data points was fit with exponential regression ($y = a + b \times e^{(c \times x)}$). P value < 0.05 was used as a criterion for statistical significance; all tests are two tailed. Data are presented as mean ± SD or as median (interquartile range). Statistical analysis was performed with the R-software (R Foundation for Statistical Computing, Austria).

Results

Prestudy data of piglets are summarized in the Supplemental Digital Content 1, http://links.lww.com/ALN/B158.

Time Course, Location, and Nature of Lung Densities

In figure 1A, we present the number of new densities (subpleural, peribronchial, and parenchymal) as a function of mechanical ventilation time in the individual piglets. As shown, the six piglets with baseline consolidated tissue (black circles) showed the same behavior as the six healthy piglets (white circles) but tended to deteriorate more rapidly. In figure 1B, we grouped all the piglets together for sake of clarity. As shown, the number of densities tended to increase exponentially in seven piglets and linearly in two piglets, whereas in three piglets, deterioration was so rapid that it was impossible to fit a curve; median time constant was 3.1 h (range, 1.5 to 3.3 h). At the last CT scan in which the new densities were distinguishable (Time 3), the subpleural lesions were more frequent (median [interquartile range], 61% [57 to 76%]) than the peribronchial and parenchymal ones (19% [11 to 23%] and 19% [6 to 25%], respectively; $P < 0.0001$ *vs.* subpleural). The details of their location (median [interquartile range]) are summarized in table 1: as shown, the densities were more frequent at the lung base than apex and hilum (46% [39 to 54%] *vs.* 21% [9 to 34%] and 29% [20 to 37%], respectively, $P < 0.01$) but similarly distributed between dependent and nondependent lung regions (48% [38 to 59%] *vs.* 52% [41 to 62%], $P = 0.11$).

New densities, one-field edema, and all-fields edema were fully recruitable and near completely cleared at end inspiration (see fig. 2). In fact the relationship between the recruitable tissue and the noninflated tissue at end expiration was close to identity indicating that what was collapsed (*i.e.*, recruitable) at end expiration opened up at end inspiration (lung recruitability, in grams = −25 + not inflated tissue at end expiration (g) × 0.90, $r^2 = 0.97$, $P < 0.0001$, see Supplemental Digital Content 1, fig. 6, http://links.lww.com/ALN/B158). This observation is reinforced by studying the time course of the densities of the six pigs with consolidated tissue at baseline. In fact, from Time 0 to Time 3, while the consolidated tissue remained constant and unrecruitable, the surrounding ventilator-induced new densities were fully recruitable at end inspiration (see fig. 3).

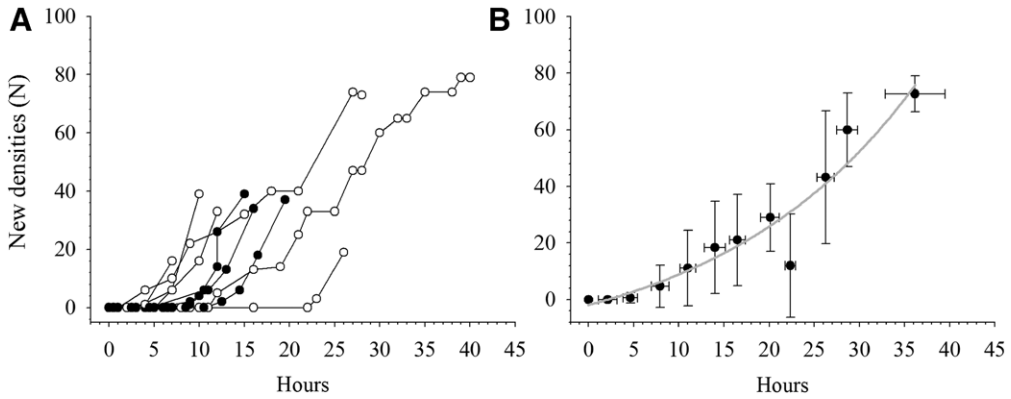

Fig. 1. Time course of new densities. (*A*) New densities (y axis) as a function of time (x axis) in individual piglets. We used all the computed tomography scans taken during the whole experiment until densities were distinguishable (time 3). Healthy pigs were represented by *white dots* and piglets with baseline abnormal densities by *black dots*. (*B*) Average number of new densities ±SD (y axis) as function of time (x axis) using 3-h intervals. We used only the computed tomography scan taken at 3-h intervals; regression was performed on average data and is purely descriptive. As behavior of individual piglets was different, we computed the time constant for seven piglets (in two piglets, the increase in new densities was linear, and in three piglets, there were not enough data points to fit a curve), and the median time constant was 3.1 h (interquartile range, 1.5 to 3.3).

Table 1. Localization of New Densities

	Subpleural	Peribronchial	Parenchymal	*P* Value
Apex	2 (1–8.5)	1 (0.75–2)	0 (0–1.25)	<0.001
Hilum	4 (2.5–7.75)	2.5 (0–4)	1.5 (0.75–2)	<0.01
Base	7.5 (5–9.5)	2 (0–3)*	3.5 (0–5.25)*	<0.0001
	16.5 (9.75–23.25)	7.5 (1–9)*	6 (3–8.75)*	<0.0001

Data are represented by number of new densities as median (interquartile range) in apex, hilum, and base at Time 3 (mixed model on the ranked variables). The two lungs of each piglet were considered together. These densities were similarly distributed between dependent and nondependent lung regions (data not shown, $P = 0.11$, see Supplemental Digital Content 1, http://links.lww.com/ALN/B158, for details).

* $P < 0.05$ *vs.* subpleural in the same row.

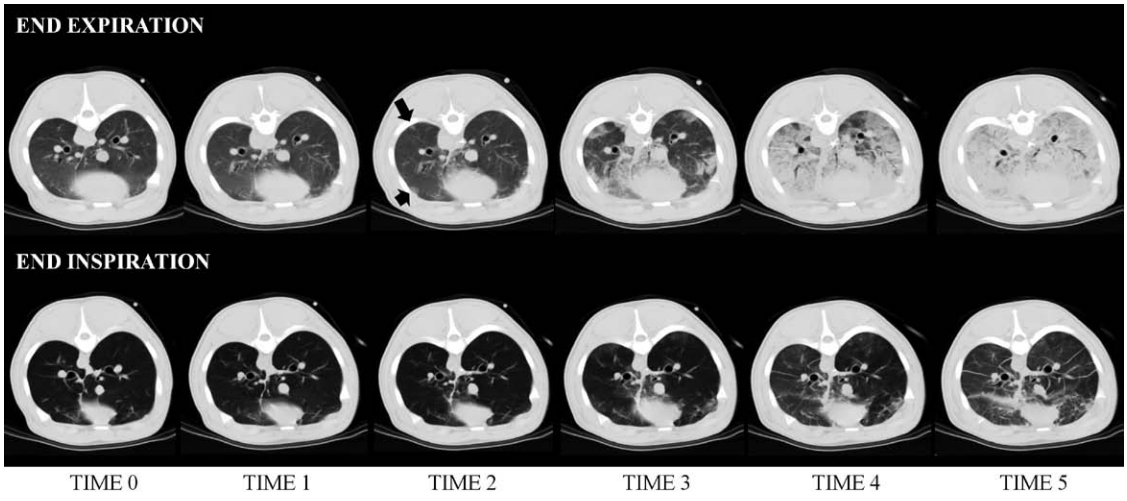

Fig. 2. Computed tomography (CT) scan time course of ventilator-induced lung injury. Representative CT scan images at end expiration (*upper row*) and at end inspiration (*lower row*) at the six study time points: Time 0 = baseline CT scan; Time 1 = last CT scan without new densities; Time 2 = first CT scan with new densities (*arrows*); Time 3 = last CT scan with distinguishable new densities; Time 4 = first CT scan with one-field edema; Time 5 = first CT scan with all-field edema.

Lung Inhomogeneities

In figure 4A, we show the time course of the lung inhomogeneities in the individual piglets. As shown, piglets with baseline consolidated tissue tended to have greater baseline inhomogeneities compared with the healthy piglets (9.5 ± 4.4% *vs.* 5.7 ± 1.6% of lung volume, $P = 0.09$). In figure 4B, the average lung inhomogeneities time course is summarized. The increase in inhomogeneity extent was fit in

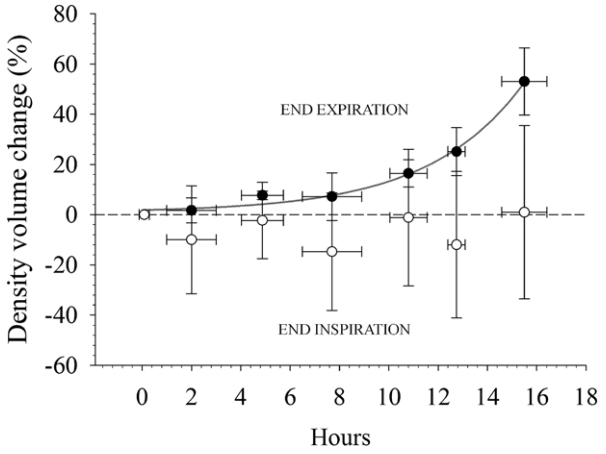

Fig. 3. Behavior of baseline abnormal lung densities. Percentage of volume change of baseline abnormal densities as a function of time at end expiration (*black dots*) and end inspiration (*white dots*). The volume of abnormal baseline densities at end-inspiration did not change significantly ($P = 0.84$), whereas it significantly increased at end-expiration ($P < 0.01$). Volume increase (%) = $0.92 + 0.91 \times e^{0.26 \times \text{hours}}$, $r^2 = 0.99$, $P < 0.0001$.

each piglet with an exponential function. Median time constant was 3.3 h (interquartile range, 2.0 to 4.4 h). In piglets without baseline densities, median time constant was 3.8 h (interquartile range, 2.4 to 5.0 h), whereas in piglets with baseline consolidated tissue, it was 2.6 h (interquartile range, 1.6 to 3.5 h; $P = 0.29$). Representative images of lung inhomogeneities time course are presented in figure 4C.

Structure–Function Relationship

Representative CT scan images from Time 0 to Time 5 are reported in figure 2. In table 2, we report the most relevant CT scan variables. As shown, lung recruitability increased significantly at Time 4. Total lung tissue increase and gas volume decrease reached statistical significance at Time 5. The changes of well, poorly, and not inflated tissue (Supplemental Digital Content 1, fig. 7, http://links.lww.com/ALN/B158) followed an exponential behavior, as well as the changes of respiratory system and lung elastance (see table 3), being the chest wall elastance near-constant through the experiment.

As shown in table 3, the gas exchange remained near-constant at baseline levels until the one-field edema developed (Time 4), whereas the oxygen saturation (FIO_2, 50%) was maintained between 95 and 100% even when all-field edema was present.

In table 3 and Supplemental Digital Content 1, table 6, http://links.lww.com/ALN/B158, we report the hemodynamic variables: the SvO_2 decreased and arterial–venous oxygen difference increased with time (Time 3). Although diuresis was always present, arterial pressure maintained,

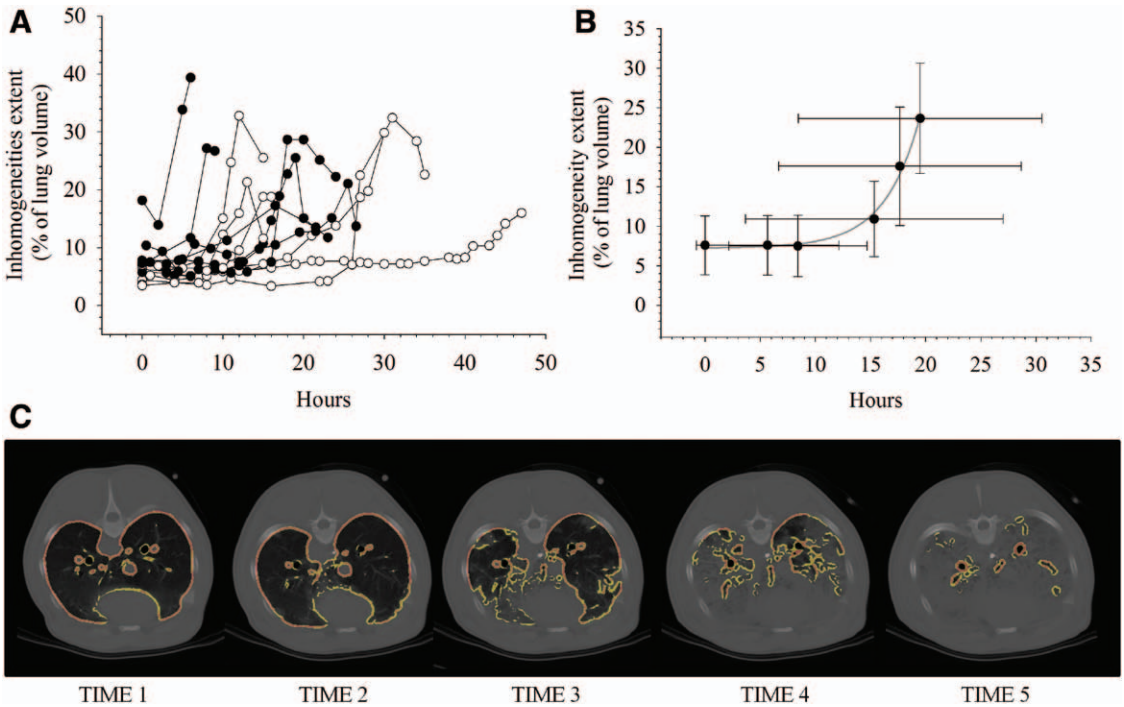

Fig. 4. Time course of lung inhomogeneities. (*A*) Extent of lung inhomogeneity (% of lung volume) as function of time in the individual pigs. Healthy pigs are represented by *white dots* and piglets with baseline abnormal densities by *black dots*. (*B*) Average lung inhomogeneity extent ±SD (y axis) as a function of the six time points ±SD (x axis). Median time constant was 3.3 h (2.0 to 4.4). In piglets without baseline densities, median time constant was 3.8 h (2.4 to 5.0), whereas in piglets with baseline consolidated tissue, it was 2.6 h (1.6 to 3.5). (*C*) False-color images of the lung inhomogeneities superimposed to computed tomography scan images of a representative pig taken from Time 1 to Time 5. *Yellow* represents lung inhomogeneities between 1.84 and 3 and *red* represents lung inhomogeneities greater than 3.

Table 2. CT Scan Data

	Baseline CT Scan (Time 0)	Last CT Scan without New Densities (Time 1)	First CT Scan with New Densities (Time 2)	Last CT Scan with Distinguishable Densities (Time 3)	First CT Scan with One-field Edema (Time 4)	First CT Scan with All-field Edema (Time 5)	*P* Value
Time (h)	0±0	5.7±6.5	8.4±6.3	15±12	18±11	20±11	
Total lung weight (g)							
End expiratory	411±82	420±93	408±87	438±80	500±141	628±268*	<0.0001
End inspiratory	402±96	385±89	368±82	402±77	464±117	636±304*	<0.0001
Lung gas volume (ml)							
End expiratory	365±108	385±158	395±159	370±133	310±108	241±69*	<0.0001
End inspiratory	1232±344	1177±166	1129±132	1070±190	1053±201*	1002±191*	<0.0001
Total volume (ml)							
End expiratory	775±133	805±216	803±213	808±184	810±194	869±309	0.33
End inspiratory	1634±384	1562±221	1497±179	1472±184	1517±232	1638±466	0.78
Recruitable tissue (g)	14±12	17±13	14±13	24±14	66±54	161±100*	<0.0001
Recruitability (% of lung tissue)	3±2.4	3.7±2.5	3.3±2.6	5.4±2.6	13±9.2*	24±8.6*	<0.0001
Volume increase of baseline lesions (%)							
End expiratory	0±0	9.3±5.9	16±13*	46±12*	—	—	<0.01
End inspiratory	0±0	–3.3±21	–10±21	–19±45	—	—	0.72

Statistical analysis was performed with a mixed model and, if the overall model was significant, all data points were compared with Time 0 (baseline) correcting the *P* values with the Bonferroni method.

* $P < 0.05$ *vs*. baseline (Time 0).

CT = computed tomography.

Table 3. Respiratory Mechanics, Hemodynamics, and Gas Exchange Variables

	Baseline CT Scan (Time 0)	Last CT Scan without New Densities (Time 1)	First CT Scan with New Densities (Time 2)	Last CT Scan with Distinguishable Densities (Time 3)	First CT Scan with One-field Edema (Time 4)	First CT Scan with All-field Edema (Time 5)	*P* Value
Time (h)	0±0	5.7±6.5	8.4±6.3	15±12	18±11	20±11	
Plateau pressure (cm H_2O)	27±3.5	28±3.3	30±5	32±4.6*	38±6.5*	41±6.5*	<0.0001
Transpulmonary pressure (cm H_2O)/lung stress	19±3	20±3.3	22±3.8	25±3.8*	30±6.1*	34±8*	<0.0001
Lung strain	3.3±0.56	3.3±0.51	3.3±0.54	3.4±0.49	4±0.9	4.7±1.2*	<0.0001
Respiratory system elastance (cm H_2O/l)	34±4.6	34±4.4	37±5.4	39±6.5	46±12*	51±11*	<0.0001
Lung elastance (cm H_2O/l)	24±3.8	24±4.6	27±5	31±5.7	38±11*	43±12*	<0.0001
Chest wall elastance (cm H_2O/l)	9.5±4.5	10±4.2	9.6±3.6	8.5±4	8.8±4.5	8±4.8	0.03
Pa_{O_2}/FI_{O_2}	508±83	511±87	510±76	490±58	415±135*	365±160*	<0.0001
Shunt (%)	7±5	7±6	5±1	5±2	7±5	9±6	0.30
Sa_{O_2} (%)	100±0	100±1	100±0	100±0	99±2	98±3*	0.02
Pa_{CO_2} (mmHg)	19±9.8	18±10	16±8.5	16±8.4	17±8.5	17±6.8	0.62
pH	7.70±0.114	7.69±0.114	7.69±0.101	7.64±0.082	7.57±0.088*	7.53±0.17*	<0.001
Base excess (mmol/l)	1.5±3.7	–0.47±5.5	–2.4±4.7	–4.5±5.4	–6.3±5.2*	–8.6±5.6*	<0.0001
Mean arterial pressure (mmHg)	92±19	87±17	93±16	87±22	81±23	82±25	0.34
Central venous pressure (mmHg)	6.3±4.5	6.6±4	7.3±3.6	7.3±3.6	8±3.3	8.1±4.1	0.10
Sv_{O_2} (%)	75±14	70±13	65±11	63±8.2*	59±12*	52±14*	<0.001
Cumulative fluid balance (ml)	570±507	880±730	851±720	974±974	1143±1109	996±1032	0.10

Statistical analysis was performed with a mixed model and, if the overall model was significant, all data points were compared with Time 0 (baseline) correcting the *P* values with the Bonferroni method.

* $P < 0.05$ *vs*. baseline (Time 0).

CT = computed tomography.

and lactates did not increased significantly, we observed a progressive metabolic acidosis from Time 1 to Time 5, as shown by the base deficit increase. In addition, the use of this extremely aggressive ventilation was associated with fluid retention and, in five pigs, required the use of vasopressors at the end of the experiment (Time 5).

Table 4. Summary of Histologic Findings

	Central Lung Regions	Peripheral Lung Regions	*P* Value
Ruptured alveoli	2.25 (1.22–2.69)	1.56 (1.31–1.88)	0.18
Interstitial infiltrate	0.81 (0.31–1.03)	0.50 (0.33–0.50)	0.21
Hyaline membranes	2.25 (1.75–2.75)	2.50 (2.12–2.50)	0.79
Infiltrate intensity	0.25 (0.19–0.53)	0.38 (0.18–0.81)	0.80
Intra-alveolar infiltrate	1.88 (1.50–2.06)	2.00 (1.81–2.19)	0.12
Erythrocytes leakage	1.50 (1.12–1.75)	0.88 (0.69–1.12)	0.03
Collagen (% of lung parenchyma)	3.60 (3.00–4.12)	4.13 (3.48–5.49)	0.09
Elastin (% of lung parenchyma)	9.45 (6.93–15.51)	8.89 (7.52–10.78)	0.22

Histologic parameters of damage (expressed as score: 0 = no alterations; 1 = 25% of field involved; 2 = 50% of field involved; 3 = 75% of field involved; 4 = 100% of field involved) and the percentage of collagen and elastin on total parenchyma for each field are shown. Values are expressed as median (interquartile range). Intra-alveolar infiltrate means presence of neutrophils in the alveolar space, intensity of the number of cells and interstitial neutrophils accumulated in the interstitial space; and erythrocytes leakage means the presence of erythrocytes outside the vessel, ruptured alveoli means discontinuation of the alveolar wall. Histologic analysis was available in seven piglets. The medians of all samples taken from the central and peripheral lung regions were computed for each piglet and compared with paired Wilcoxon test. Details of lung sampling are reported in the Supplemental Digital Content 1, http://links.lww.com/ALN/B158.

Histology

Macroscopic Anatomy. At autopsy, the lungs appeared heavy, purple, and congested; however, when inflated outside, the chest wall appeared near-normal (pinky and well inflated). Autoptic lung weight was 626 ± 252 g (baseline CT scan computed lung weight, 411 ± 82 g), and median wet-to-dry ratio was 7.54 (6.72 to 8.27) confirming the presence of diffuse edema; we did not find difference in wet-to-dry ratio between the lung regions sampled.

Microscopic Anatomy. Histologic analyses, available in seven pigs, are summarized in table 4. As shown, the different pathologic findings were similarly distributed between the central and the peripheral lung regions except for erythrocytes leakage that was more represented in the central lung regions. The collagen was significantly more represented in the peripheral than in the central samples. The pathologic findings are primarily in the extracellular matrix, being the intra-alveolar space relatively spared: The median ratio of alveolar to interstitial infiltrate was 0.18 (0.15 to 0.24) (see Supplemental Digital Content 1, http://links.lww.com/ALN/B158, for details).

Discussion

The main finding of this study is that in an experimental model of lethal mechanical ventilation obtained applying very high stress and strain to the lung parenchyma, abnormal lung densities first develop at the interface between structures with different extensibility, in line with the hypothesis of "stress raisers"–associated inhomogeneities.[16,17] The number of new densities increases exponentially with time up to all-field lung edema. In addition, all the new densities are fully recruitable, suggesting that pulmonary units are collapsed instead of consolidated.

In this study, we used an extremely aggressive "lethal ventilation" by inducing a lung strain greater than 2.5,[19] which corresponded in these animals to approximately 40 ml/kg, a value known to induce lethal VILI in several animal species.[8–10] The plateau pressures (27 ± 3.5 cm H_2O) and the end-inspiratory transpulmonary pressures (19 ± 3 cm H_2O) were used in these pigs to reach or exceed the total lung capacity at each breath. In fact, the specific elastance of normal piglets is about half than in humans (~6 *vs.* ~12 cm H_2O).[23] At the interface between structures of different distensibility or geometry, as bronchi/vessels and neighboring alveoli or the visceral pleura[18] and the alveolar walls departing from it, the applied pressure may lead to stress concentration ("stress raiser").

The parenchymal stress, locally amplified by the "stress raisers," may lead with time to the rupture of extracellular polymers as proteoglycan and hyaluronan, which, in turn, may act as a trigger for inflammatory reaction,[24] as well as to a rupture of capillaries with erythrocytes extravasation.[4,25] In addition, the excessive tidal strain may be associated with a decrease of surfactant activity.[26] All these phenomena justify the increase of densities we observed. With this kind of ventilation, we found a specific elastance greater than we previously observed[19] (10 ± 3.2 cm H_2O *vs.* 5.4 ± 2.2 cm H_2O). This may be due to the extracellular matrix overstretch (as we measured the elastance by using extremely large tidal volumes), but it is also compatible with a surfactant decrease and structural alterations of the extracellular matrix.

The ventilator-induced lung densities were fully recruitable during inspiration (see figs. 3 and 4). This full recruitability strongly suggests that the pathologic processes induced by the mechanical ventilation are primarily located in extracellular matrix leading to pulmonary units collapse instead of consolidation. Actually, histologic findings showed that the pathologic processes primarily occurred in the interstitial space instead than in alveolar space. That VILI primarily occurs in the interstitial space and is further sustained by the observation that the consolidated tissue present at baseline in 6 of the 12 pigs remained of the same size throughout the experiment, while in the meantime, at its interface, recruitable densities developed (see fig. 3).

The anatomical lung alterations fully accounted for the progressive increase in lung elastance observed with time. Although in human ARDS, the increase in lung elastance is

primarily due to the decreased size of the lung open to ventilation,[27] being the specific elastance in normal range (the "baby lung"[28]), in this model, the concept of "baby lung" does not apply as, at the end inspiration, the whole lung is open to ventilation. Therefore, the increased elastance in this model reflects, more than the lung size, the "extra pressure" required, during inflation, to overcome the alteration of the extracellular matrix (increased specific elastance) and to overcome the opening pressures of the collapsed pulmonary units.

There is extensive evidence that pH may modulate the development of VILI, being acidosis protective[12,29] and alkalosis detrimental.[30] In this study, the severe hypocapnia was due to the extremely large tidal volumes used. We chose, for simplicity, to maintain this strategy as in a previous study[19];we found that hypocapnic animals and animals maintained with normal Pa_{CO_2} by an artificial dead space had the same strain threshold for the development of VILI. Compared with other variables, the oxygenation changed less: even with all-field edema and the well-aerated tissue at end expiration lower than 10%, the average Pa_{O_2}/F_{IO_2} was 365. To explain the different time course of oxygenation, compared with CT anatomy and lung mechanics, we may consider two factors: first, during the inspiratory time, the lung was completely open and gas exchange could take place; second, the hypoxic vasoconstriction could be still effective, as documented in human ARDS, where oxygenation was maintained near-constant with a noninflated tissue ranging from 20 to 50% of total lung weight.[31]

Our results underline the close relationship among lung inhomogeneities, anatomical deterioration, and clinical symptoms. In addition, they support, although not prove, the stress raiser hypothesis,[16,17] appearing more as a "proof of the concept" than a reality transferrable as such to the human being. In fact, in human ARDS, the subpleural densities are uncommon, likely because the inhomogeneities in the ARDS parenchyma far exceed quantitatively the inhomogeneities between alveoli, visceral pleura, vessels, and bronchi. Accordingly, we must note that the densities present at the baseline in six pigs increased their volume already at Time 1, well before the subpleural densities appearance at Time 2.

We think that the full recruitability of these VILI-induced densities deserves some comment: in fact, in human ARDS, we observed that the same amount of consolidated tissue could be associated with small amount of recruitable tissue (~5% lower recruiters, low severity/mortality) or considerable amount of recruitable tissue (~30% higher recruiters, high severity/mortality).[22] Although the difference in amount of recruitable tissue, being the "core" consolidated tissue similar in higher and lower recruiters, may be due to a different "loss of compartmentalization" or different spreading of inflammatory mediators, we cannot exclude that inappropriate mechanical ventilation could have contributed to the recruitability pattern.

Finally, we do not have an explanation of a constant phenomenon we observed in this VILI models: the exponential anatomic and physiologic deterioration after a variable time of latency, in both healthy pigs and in the ones with baseline consolidated tissue, where the processes were accelerated. This exponential deterioration is not observed in clinical practice[32]; we ignore the mechanisms, but it is possible that the progression of VILI in human ARDS is prevented or dampened by coexisting reparative processes.

This study was designed to support the concept that inhomogeneities are possibly related to the concentration of stress, and our results confirm the hypothesis, as the lesions actually occurred where inhomogeneities are normally present. However, to reach the result we had to use very large tidal volumes, as the inhomogeneities are very scarcely represented in normal lungs.[17] In the animals with pathologic lung densities at baseline (greater percentage of inhomogeneity in the lung parenchyma), the injuries developed first at the interface between the pathologic densities and normal parenchyma. Therefore, with this study, we may conclude that the stress raisers[16] likely exist. The presence of stress raisers should imply a greater attention in tailoring a "gentle" mechanical ventilation, as transpulmonary pressure level, safe if applied in normal lungs, if locally multiplied nearly twofold, as we found in ARDS, may end up with stress/strain leading to VILI in the ventilable lung.

Acknowledgments

The authors thank Mrs. Gabriella Trudu and Mrs. Patrizia Minunno (Dipartimento di Anestesia, Rianimazione ed Emergenza Urgenza, Fondazione IRCCS Ca' Granda-Ospedale Maggiore Policlinico, Milan, Italy) for invaluable logistic support; Mr. Fabio Ambrosetti (Dipartimento di Fisiopatologia Medico-Chirurgica e dei Trapianti, Fondazione IRCCS Ca' Granda-Ospedale Maggiore Policlinico, Università degli Studi di Milano, Milan, Italy) for technical assistance; Daniela Febres, M.D., Greta Rossignoli, M.D., Elisabetta Gallazzi, M.D., Antonella Marino, M.D., and Thomas Langer, M.D. (Dipartimento di Fisiopatologia Medico-Chirurgica e dei Trapianti, Fondazione IRCCS Ca' Granda-Ospedale Maggiore Policlinico, Università degli Studi di Milano, Milan, Italy), and Alberto Zanella, M.D. (Dipartimento di Scienze della Salute Università di Milano Bicocca, Ospedale San Gerardo Nuovo dei Tintori, Monza, Italy), for their support in the conduction of experiments; Luciano Lombardi, M.D., Massimo Monti, M.D., and Beatrice Comini, M.D. (Dipartimento di Anestesia, Rianimazione ed Emergenza Urgenza, Fondazione IRCCS Ca' Granda-Ospedale Maggiore Policlinico, Milan, Italy), and Davide Zani, D.V.M., Giuliano Ravasio, D.V.M., Mauro Di Giancamillo, D.V.M. (Dipartimento di Scienze Veterinarie e Sanità Pubblica, Università degli Studi di Milano, Milan, Italy), for technical assistance with computed tomography scan images; and Paolo Cadringher, M.Sc. (Dipartimento di Anestesia, Rianimazione ed Emergenza Urgenza, Fondazione IRCCS Ca' Granda-Ospedale Maggiore Policlinico, Milan, Italy), for software development.

Support was provided from institutional and/or departmental sources and supported in part by an Italian grant

provided by Fondazione Fiera di Milano (Milan, Italy) for Translational and Competitive Research (2007, Dr. Gattinoni) and by the ESICM Bernhard Dräger Award for Advanced Treatment of Acute Respiratory Failure (ESICM, Brussels, Belgium) to Dr. Cressoni.

Competing Interests

Drs. Cressoni and Gattinoni have applied for a patent for the stress raisers quantification: "Method for determining inhomogeneity in a portion of animal tissue, involves identifying space surrounding central voxel and containing peripheral voxels group and obtaining multiple values of peripheral and central voxel densities." Italian patent granted: N. ITCO20110062, on June 14, 2013; European and U.S. patent application filled: WO 2013/088336 A1. Patent assignee: Fondazione IRCCS Ca' Granda-Ospedale Maggiore Policlinico. Inventor(s): Luciano Gattinoni, Paolo Cadringher, and Massimo Cressoni. The other authors declare no competing interests.

Correspondence

Address correspondence to Dr. Gattinoni: Dipartimento di Anestesia, Rianimazione ed Emergenza Urgenza, Fondazione IRCCS Ca' Granda – Ospedale Maggiore Policlinico, Via Francesco Sforza 35, 20122 Milan, Italy. gattinon@policlinico.mi.it. Information on purchasing reprints may be found at www.anesthesiology.org or on the masthead page at the beginning of this issue. Anesthesiology's articles are made freely accessible to all readers, for personal use only, 6 months from the cover date of the issue.

References

1. Ventilation with lower tidal volumes as compared with traditional tidal volumes for acute lung injury and the acute respiratory distress syndrome. The Acute Respiratory Distress Syndrome Network. N Engl J Med 2000; 342:1301–8
2. Ranieri VM, Suter PM, Tortorella C, De Tullio R, Dayer JM, Brienza A, Bruno F, Slutsky AS: Effect of mechanical ventilation on inflammatory mediators in patients with acute respiratory distress syndrome: A randomized controlled trial. JAMA 1999; 282:54–61
3. Futier E, Constantin JM, Paugam-Burtz C, Pascal J, Eurin M, Neuschwander A, Marret E, Beaussier M, Gutton C, Lefrant JY, Allaouchiche B, Verzilli D, Leone M, De Jong A, Bazin JE, Pereira B, Jaber S; IMPROVE Study Group: A trial of intraoperative low-tidal-volume ventilation in abdominal surgery. N Engl J Med 2013; 369:428–37
4. Marini JJ, Hotchkiss JR, Broccard AF: Bench-to-bedside review: Microvascular and airspace linkage in ventilator-induced lung injury. Crit Care 2003; 7:435–44
5. Broccard AF, Hotchkiss JR, Kuwayama N, Olson DA, Jamal S, Wangensteen DO, Marini JJ: Consequences of vascular flow on lung injury induced by mechanical ventilation. Am J Respir Crit Care Med 1998; 157(6 pt 1):1935–42
6. Broccard AF, Vannay C, Feihl F, Schaller MD: Impact of low pulmonary vascular pressure on ventilator-induced lung injury. Crit Care Med 2002; 30:2183–90
7. Suzuki S, Hotchkiss JR, Takahashi T, Olson D, Adams AB, Marini JJ: Effect of core body temperature on ventilator-induced lung injury. Crit Care Med 2004; 32:144–9
8. Dreyfuss D, Saumon G: Ventilator-induced lung injury: Lessons from experimental studies. Am J Respir Crit Care Med 1998; 157:294–323
9. Kolobow T, Moretti MP, Fumagalli R, Mascheroni D, Prato P, Chen V, Joris M: Severe impairment in lung function induced by high peak airway pressure during mechanical ventilation. An experimental study. Am Rev Respir Dis 1987; 135:312–5
10. Dreyfuss D, Basset G, Soler P, Saumon G: Intermittent positive-pressure hyperventilation with high inflation pressures produces pulmonary microvascular injury in rats. Am Rev Respir Dis 1985; 132:880–4
11. Hernandez LA, Coker PJ, May S, Thompson AL, Parker JC: Mechanical ventilation increases microvascular permeability in oleic acid-injured lungs. J Appl Physiol (1985) 1990; 69:2057–61
12. Sinclair SE, Altemeier WA, Matute-Bello G, Chi EY: Augmented lung injury due to interaction between hyperoxia and mechanical ventilation. Crit Care Med 2004; 32:2496–501
13. Altemeier WA, Matute-Bello G, Gharib SA, Glenny RW, Martin TR, Liles WC: Modulation of lipopolysaccharide-induced gene transcription and promotion of lung injury by mechanical ventilation. J Immunol 2005; 175:3369–76
14. Costa EL, Musch G, Winkler T, Schroeder T, Harris RS, Jones HA, Venegas JG, Vidal Melo MF: Mild endotoxemia during mechanical ventilation produces spatially heterogeneous pulmonary neutrophilic inflammation in sheep. Anesthesiology 2010; 112:658–69
15. Wellman TJ, Winkler T, Costa EL, Musch G, Harris RS, Zheng H, Venegas JG, Vidal Melo MF: Effect of local tidal lung strain on inflammation in normal and lipopolysaccharide-exposed sheep*. Crit Care Med 2014; 42:e491–500
16. Mead J, Takishima T, Leith D: Stress distribution in lungs: A model of pulmonary elasticity. J Appl Physiol 1970; 28:596–608
17. Cressoni M, Cadringher P, Chiurazzi C, Amini M, Gallazzi E, Marino A, Brioni M, Carlesso E, Chiumello D, Quintel M, Bugedo G, Gattinoni L: Lung inhomogeneity in patients with acute respiratory distress syndrome. Am J Respir Crit Care Med 2014; 189:149–58
18. Luque T, Melo E, Garreta E, Cortiella J, Nichols J, Farré R, Navajas D: Local micromechanical properties of decellularized lung scaffolds measured with atomic force microscopy. Acta Biomater 2013; 9:6852–9
19. Protti A, Cressoni M, Santini A, Langer T, Mietto C, Febres D, Chierichetti M, Coppola S, Conte G, Gatti S, Leopardi O, Masson S, Lombardi L, Lazzerini M, Rampoldi E, Cadringher P, Gattinoni L: Lung stress and strain during mechanical ventilation: Any safe threshold? Am J Respir Crit Care Med 2011; 183:1354–62
20. National Research Council (U.S.), Institute for Laboratory Animal Research (U.S.), National Academies Press (U.S.): Guide for the Care and Use of Laboratory Animals, 8th edition. Washington, D.C, National Academies Press, 2011
21. www.elekton.it. Accessed April 1, 2015.
22. Gattinoni L, Caironi P, Cressoni M, Chiumello D, Ranieri VM, Quintel M, Russo S, Patroniti N, Cornejo R, Bugedo G: Lung recruitment in patients with the acute respiratory distress syndrome. N Engl J Med 2006; 354:1775–86
23. Chiumello D, Carlesso E, Cadringher P, Caironi P, Valenza F, Polli F, Tallarini F, Cozzi P, Cressoni M, Colombo A, Marini JJ, Gattinoni L: Lung stress and strain during mechanical ventilation for acute respiratory distress syndrome. Am J Respir Crit Care Med 2008; 178:346–55
24. Jiang D, Liang J, Fan J, Yu S, Chen S, Luo Y, Prestwich GD, Mascarenhas MM, Garg HG, Quinn DA, Homer RJ, Goldstein DR, Bucala R, Lee PJ, Medzhitov R, Noble PW: Regulation of lung injury and repair by Toll-like receptors and hyaluronan. Nat Med 2005; 11:1173–9
25. Marini JJ: Microvasculature in ventilator-induced lung injury: Target or cause? Minerva Anestesiol 2004; 70:167–73
26. Verbrugge SJ, Böhm SH, Gommers D, Zimmerman LJ, Lachmann B: Surfactant impairment after mechanical ventilation with large alveolar surface area changes and effects

of positive end-expiratory pressure. Br J Anaesth 1998; 80:360–4

27. Gattinoni L, Pesenti A, Bombino M, Baglioni S, Rivolta M, Rossi F, Rossi G, Fumagalli R, Marcolin R, Mascheroni D: Relationships between lung computed tomographic density, gas exchange, and PEEP in acute respiratory failure. Anesthesiology 1988; 69:824–32
28. Gattinoni L, Pesenti A: The concept of "baby lung". Intensive Care Med 2005; 31:776–84
29. Peltekova V, Engelberts D, Otulakowski G, Uematsu S, Post M, Kavanagh BP: Hypercapnic acidosis in ventilator-induced lung injury. Intensive Care Med 2010; 36:869–78
30. Mascheroni D, Kolobow T, Fumagalli R, Moretti MP, Chen V, Buckhold D: Acute respiratory failure following pharmacologically induced hyperventilation: An experimental animal study. Intensive Care Med 1988; 15:8–14
31. Cressoni M, Caironi P, Polli F, Carlesso E, Chiumello D, Cadringher P, Quintel M, Ranieri VM, Bugedo G, Gattinoni L: Anatomical and functional intrapulmonary shunt in acute respiratory distress syndrome. Crit Care Med 2008; 36:669–75
32. Gattinoni L, Bombino M, Pelosi P, Lissoni A, Pesenti A, Fumagalli R, Tagliabue M: Lung structure and function in different stages of severe adult respiratory distress syndrome. JAMA 1994; 271:1772–9

ANESTHESIOLOGY REFLECTIONS FROM THE WOOD LIBRARY-MUSEUM

Labat and the Anglo-French Drug Company's Neocaine

Manufactured in Paris, France, by the Corbière Laboratories (*lower right*), "PURE FRENCH NÉOCAÏNE" was a brand of the local anesthetic procaine distributed as crystals inside a glass ampoule (*high middle*) from New York City by the Anglo-French Drug Company (AFDC). Following World War I, America's brief unhappiness with using German products (*e.g.,* Novocaine) and the advocacy for Neocaine by French-trained Louis Gaston Labat, M.D. (1876–1934), combined to propel sales of Neocaine with Labat's name on the box (*high left*). By 1930 the AFDC was distributing a 22-page publication, *The Safety of Spinal Anesthesia: Labat's Technique with Neocaine,* which noted that it was "Written by a Registered Physician and Reviewed by an Authority on Spinal Anesthesia." In a 1936 advertisement, the AFDC characterized Neocaine in the "field of spinal anesthesia" as "unequaled" and compared the product to British Guiana's Kaieteur Falls, the world's broadest single-drop waterfall. During World War II as America joined British and French allies, "Anglo-French" trumpeted that "Neocaine has accompanied our armies to all parts of the world." (Copyright © the American Society of Anesthesiologists, Inc.)

George S. Bause, M.D., M.P.H., Honorary Curator, ASA's Wood Library-Museum of Anesthesiology, Schaumburg, Illinois, and Clinical Associate Professor, Case Western Reserve University, Cleveland, Ohio. UJYC@aol.com.